Journal of Robotics and Control (JRC)
Volume 6, Issue 4, 2025
ISSN: 2715-5072, DOI: 10.18196/jrc.v6i4.26229

The Effect of Eye Shape and the Use of Corrective Glasses on the Spatial Accuracy of Eye-Gaze-Based Robot Control with a Static Head Pose

Engelbert Harsandi Erik Suryadarma [1], Pringgo Widyo Laksono [2*], Ilham Priadythama [3], Lobes Herdiman [4], Muhammad Syaiful Amri Bin Suhaimi [5]
[1, 2, 3, 4] Department of Industrial Engineering, Universitas Sebelas Maret, Surakarta, Indonesia
[1] Department of Industrial Engineering, Universitas Atma Jaya Yogyakarta, Yogyakarta, Indonesia
[5] Faculty of Information and Communication Technology, Universiti Tunku Abdul Rahman, Kampar, Malaysia
Email: [1] engelbert.harsandi@uajy.ac.id, [2] pringgo@ft.uns.ac.id, [3] priadythama@gmail.com, [4] lobesherdiman@staff.uns.ac.id, [5] syaifulamri@utar.edu.my
*Corresponding Author

***Abstract*—The integration of eye-gaze technology into robotic control systems has shown considerable promise in enhancing human–robot interaction, particularly for individuals with physical disabilities. This study investigates the influence of eye morphology and the use of corrective eyewear on the spatial accuracy of gaze-based robot control under static head pose conditions. Experiments were conducted using advanced eye-tracking systems and multiple machine learning algorithms—decision tree, support vector machine, discriminant analysis, naïve bayes, and K-nearest neighbor—on a participant pool with varied eye shapes and eyewear usage. The experimental design accounted for potential sources of bias, including lighting variability, participant fatigue, and calibration procedures. Statistical analyses revealed no significant differences in gaze estimation accuracy across eye shapes or eyewear status. However, a consistent pattern emerged: participants with non-monolid eye shapes achieved, on average, approximately 1% higher accuracy than those with monolid eye shapes—a difference that, while statistically insignificant, warrants further exploration. The findings suggest that gaze-based robotic control systems can operate reliably across diverse user groups and hold strong potential for use in assistive technologies targeting individuals with limited mobility, including those with severe motor impairments such as head paralysis. To further enhance the inclusiveness and robustness of such systems, future research should explore additional anatomical variations and environmental conditions that may influence gaze estimation accuracy.**

Keywords—Eye Shape; Static Head Pose; Gaze Estimation Algorithms; Robot Control; Human-Robot Interaction; Inclusive Design.

I. INTRODUCTION

The rapid advancement of robotic technology has significantly transformed various sectors, including healthcare, manufacturing, and education [1]–[4]. Robotics has become an integral part of modern industry, driving automation, efficiency, and precision in diverse applications [5]–[10]. One of the most promising innovations in this field is the integration of eye-gaze technology, which allows users to control robotic systems through their eye movements [11]–[16].

The integration of eye-gaze technology into robotic control systems represents a transformative advancement in human-robot interaction, with significant implications for assistive technologies [17]–[22]. For individuals with severe physical disabilities, such as tetraplegia, amyotrophic lateral sclerosis (ALS), or cerebral palsy, conventional interaction modalities, such as joystick-based or speech-based control, are often infeasible or inadequate [23]–[27]. In such contexts, eye-gaze control offers a direct, intuitive, and non-invasive alternative that enables users to manipulate robotic devices and digital interfaces using only their eye movements. This capability not only promotes greater autonomy and quality of life but also holds potential for expanding access to education, employment, and social participation for individuals with mobility impairments.

Eye gaze estimation, a core component of gaze-based robotic control, has garnered increasing attention in recent years [28]–[32]. This technology relies on sophisticated computer vision techniques and machine learning algorithms to track and interpret eye movements with high precision [33]–[35]. Over time, researchers have focused on refining gaze estimation techniques to overcome challenges such as variations in lighting conditions, head movements, and anatomical differences among users [36]–[37]. One critical research area within gaze estimation is its application in human-robot interaction (HRI), particularly in social robotics[38]–[44]. Studies have explored how robots can utilize gaze information to assess human attention, infer intentions, and facilitate seamless communication, thereby enhancing collaborative human-robot interactions [45]–[47]. By incorporating gaze-based control mechanisms into social robotics, researchers aim to develop robots that can respond more effectively to human behavior, particularly in service-oriented environments, such as healthcare and customer assistance [48]–[54].

At the core of gaze-based control systems lies the task of accurately estimating the user's gaze direction [55]–[59]. Contemporary eye-tracking technologies leverage a combination of computer vision techniques and machine learning algorithms to capture and interpret eye movements with high spatial and temporal resolution [60]–[65]. Over the

past decade, significant strides have been made in improving the robustness of gaze estimation under varying conditions, including head movements, lighting variations, and environmental noise [66]–[70].

Furthermore, the versatility of eye-tracking has been demonstrated across multiple domains beyond assistive technologies [71]–[75]. In social robotics, gaze information is employed to facilitate joint attention, infer human intentions, and improve the fluidity of human-robot communication [76]–[81]. Similarly, in virtual and augmented reality applications, gaze-tracking enables intuitive navigation, object interaction, and context-aware computing [82]–[84]. These diverse applications underscore the technological maturity and expanding relevance of gaze estimation systems.

Despite these advances, several human-centered factors continue to pose challenges to the accuracy and inclusiveness of gaze-tracking technologies. One such critical factor is anatomical variability in eye morphology [85]–[88]. Differences in eyelid structure, palpebral fissure width, epicanthic folds, and scleral exposure have been shown to influence the performance of gaze estimation algorithms. For instance, individuals with monolid eyes—a common trait in East Asian populations—typically exhibit reduced sclera visibility and altered eye contours, potentially impairing feature extraction processes. Similarly, the use of corrective eyewear introduces optical distortions, reflections, and calibration difficulties that can further degrade tracking accuracy.

While these challenges have been acknowledged in literature, several methodological limitations persist in prior studies. First, most investigations examining the impact of eye morphology or the use of eyewear on gaze estimation have employed small, homogeneous participant samples, often lacking balanced representation of monolid and non-monolid eye shapes or varying eyewear types. Second, many studies have focused solely on static gaze estimation tasks, such as screen-based fixation or target selection, without extending evaluation to spatially oriented tasks relevant for robotic control. Third, prior work frequently relied on highly controlled laboratory environments, neglecting realistic variability in lighting, calibration drifts, or user fatigue—factors that substantially affect real-world system performance [89]–[92]. Moreover, comparative analyses of multiple machine learning algorithms applied to anatomically diverse datasets remain scarce, limiting the understanding of how algorithmic choices interact with human variability.

These methodological limitations not only constrain the generalizability of prior findings but also hamper the development of gaze-based control systems that are robust and inclusive across diverse user populations. The inconsistent evidence regarding the influence of eye shape and the use of eyewear on gaze estimation accuracy further reinforces the need for a systematic, comprehensive investigation.

To address these gaps, it is essential to systematically evaluate how eye morphology and the use of corrective eyewear jointly influence spatial accuracy in robotic tasks. Studies must employ diversified participant samples, realistic task scenarios, and comparative algorithmic analyses to yield actionable insights for interface design and algorithm development. Leveraging machine learning classifiers, including decision tree, support vector machine, discriminant analysis, naïve bayes, and K-nearest neighbors classifiers, offers a practical approach to the empirical quantification of classification accuracy under the influence of varied human factors. These classifiers are particularly relevant due to their capability to handle heterogeneous feature spaces and to model non-linear relationships between gaze features and target locations, thus directly addressing the technical challenges posed by anatomical and optical variations.

Based on prior literature and theoretical rationale, we hypothesized that (H_0) there is no statistically significant difference in gaze estimation accuracy across users with different eye shapes or eyewear statuses; and that (H_1) non-monolid eye shapes and the absence of glasses will exhibit a marginally higher average accuracy in spatial gaze-based robot control tasks. To test these hypotheses, this study investigated the impact of eye morphology and the use of corrective glasses on the spatial accuracy of gaze-based robot control under a static head pose condition. Experiments were conducted using advanced eye-tracking systems and five machine learning algorithms, with a stratified participant pool balanced for eye shape and eyewear status.

By empirically evaluating these factors through a rigorously designed and methodologically robust study, this research contributes to advancing human-centered design in gaze-controlled robotics. The findings are expected to provide actionable insights for improving the inclusivity, adaptability, and performance of assistive technologies across diverse user populations and deployment scenarios.

In this study, we evaluated the impact of eye shape and the use of glasses on the accuracy of gaze-based robot control under a static head pose condition. A total of five machine learning algorithms were tested on gaze data from participants with varying anatomical characteristics and visual aid statuses. The findings reveal that gaze estimation accuracy remained consistent across different groups, underscoring the feasibility of inclusive gaze-driven control systems. These results contribute to the development of assistive technologies that are robust across diverse user profiles.

The research contribution of this paper takes the form of an investigation of how eye shape variations and the use of eyeglasses influence the accuracy of eye gaze estimation algorithms in a human-cyber physical system interface and the development of an evaluation framework that systematically analyzes these effects using real-user data.

II. RESEARCH DESIGN

The experiment was conducted with 24 research participants. Twelve participants wore glasses, and the rest did not. Twelve were male and the rest were female, twelve had monolid eyes and the rest had non-monolid eyes. All participants were healthy adults aged between 19 and 21 years. They had normal or corrected-to-normal vision and no known ocular or neurological impairments. They were recruited and tested in a random sequence to minimize

potential temporal confounds, such as time-of-day effects or equipment drifts. Specifically, data collection did not follow a sequential participant ID order (1-1 to 8-3), but participants were scheduled randomly across available sessions. The combination of research participants can be seen in Fig. 1. The first research participant in scenario 1 was identified as ID 1-1, the second research participant in scenario 1 was identified as ID 1-2, and so on until scenario 8, in which case the third research participant was identified as ID 8-3.

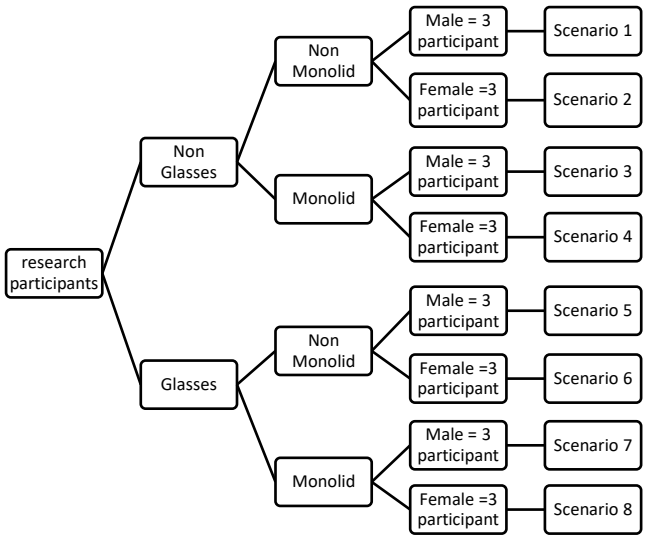

Fig. 1. The scenario of research participants

The experiment setup was arranged as shown in Fig. 2. The research participants sit on chairs facing the target in the form of a storage rack. The storage rack had nine lockers, with locker number 1 located in the center of the storage rack. In front of an operator was placed an Omron HVC-P camera module. The position of the eyes, the position of the camera and the position of rack 1 were parallel, namely at the y-axis position = 0 and the z-axis position = 0. In three-dimensional coordinates, as depicted in Fig 3, the nasal bridge was at (0,0,0) the camera was at (-50,0,0), and the center of rack 1 was at (-100,0,0) in cm. A description of the Euler angles is provided in Fig. 4.

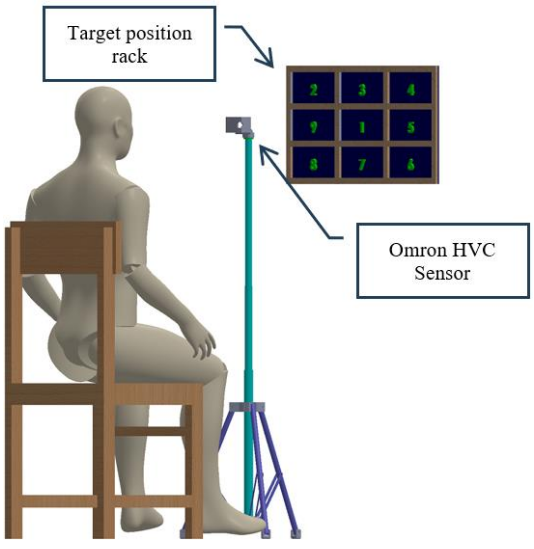

Fig. 2. Experiment setup

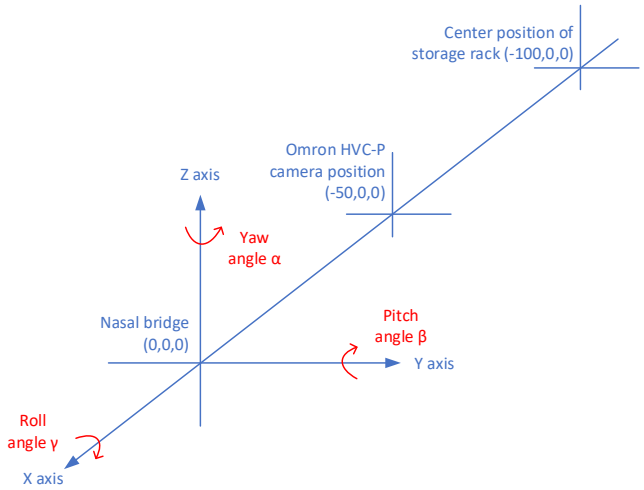

Fig. 3. Experiment setup coordinate

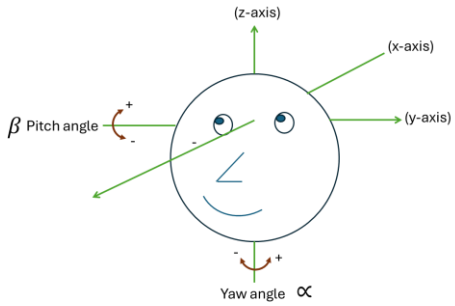

Fig. 4. Description of Euler angle

All experiments were conducted in a controlled indoor laboratory environment. Ambient lighting conditions were standardized using consistent artificial illumination and a neutral-colored background. To ensure lighting stability, ambient illuminance was continuously monitored using a calibrated lux meter. For each participant session, 60 illuminance measurements were recorded prior to data collection, immediately after each participant changeover, to confirm consistent lighting conditions across sessions. The recorded illuminance remained highly stable, with a mean of approximately 429 lux and minimal variability across all sessions. Fig. 5 shows the interval plot of lighting conditions measured across participants, indicating narrow 95% confidence intervals.

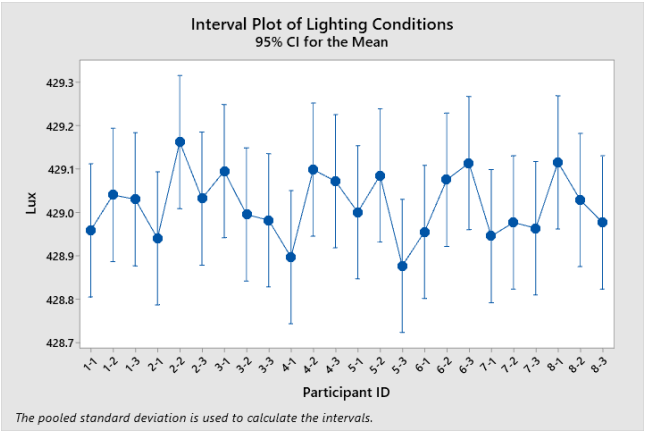

Fig. 5. Interval plot of lighting conditions (measured in lux) across all participants

In this study, the yaw and pitch angles obtained from the Omron HVC-P camera module were transformed into Cartesian coordinates using Euler angle transformations. To ensure the robustness of this process and minimize potential inaccuracies typically associated with Euler angles, several strategies were applied.

First, the participants' head movements were constrained through ergonomic positioning and explicit instructions to maintain a stable head posture. The Omron camera was aligned at eye level and at a fixed distance, minimizing extraneous head pose variations. Second, a zero-roll angle assumption was adopted in the Euler transformation model. This simplification, justified by experimental constraints and observed participant behaviours, effectively eliminated the risk of gimbal lock and reduced computational complexity in the transformation matrix. Third, a moving average filter (window size = three samples) was applied to smooth the raw yaw and pitch angles prior to coordinate transformations. This step reduced high-frequency noise while preserving gaze trajectory fidelity.

In experimental scenario 1-8, the participants were asked to direct their gaze to several lockers available in front of them without moving their necks (static head pose). The experimental procedure followed a structured flow, as illustrated in Fig. 6. The process began with the participants setting their position while ensuring they maintained a static head pose. To prevent an unintended movement, they were instructed to avoid moving their necks throughout the experiment.

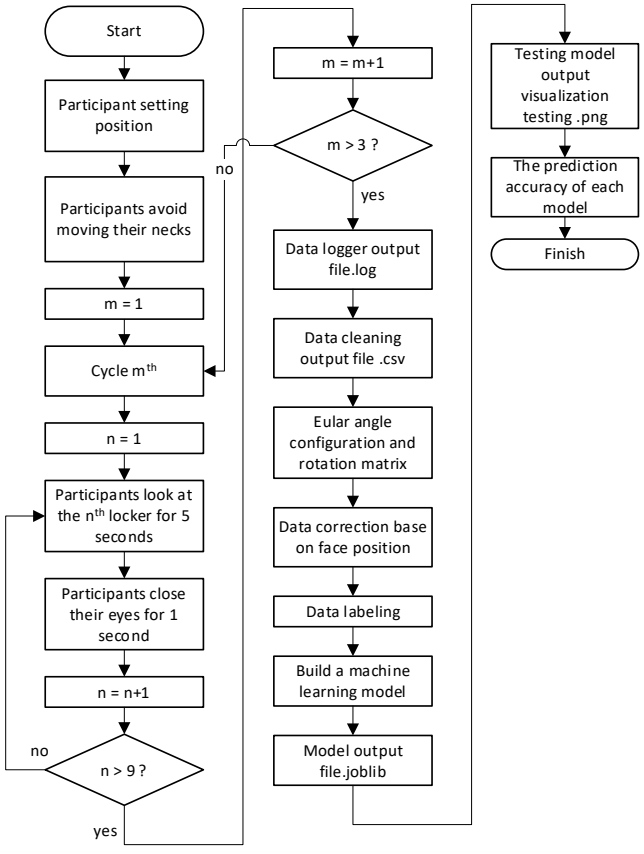

Fig. 6. Data collection and processing flowchart

The experiment followed a cyclic approach, where the cycle count (m) was initially set to 1. Within each cycle, the participants directed their gaze at the n^{th} locker for five seconds, allowing the system to record their eye movement data. After focusing on a locker, the participants closed their eyes for one second to reset their gaze before proceeding to the next locker. The locker index (n) was incremented, and this process continued until n > 9, indicating that all lockers were observed. Once a cycle was completed, m was increased, and the experiment continued until each participant completed three full cycles (m > 3).

The raw gaze data that had been collected underwent a series of processing steps to ensure accuracy and usability. First, the system generated a data logger output file (.log), which contained the recorded eye movement data. This raw data was then refined through a data cleaning process, converting it into a structured .csv file and filtering out any inconsistencies. Next, Euler angle configuration and rotation matrix calculations were performed to standardize the gaze angles and transform them into spatial coordinates. Additionally, data extraction based on facial position ensured that only valid gaze data was retained. A data labelling step followed, assigning corresponding labels to each gaze position to create a structured dataset for machine learning applications.

Once the data was all processed, a machine learning model was built to predict gaze positions based on the collected information. The trained model produced an output file (.joblib) for further analysis and implementation. To assess its performance, an output visualization file (testing.png) was generated, displaying the predicted versus actual gaze coordinates. Finally, the prediction accuracy of each model was evaluated and reported, marking the conclusion of the experiment. This systematic approach ensured a robust and structured method for collecting, processing, and analyzing gaze-based control data, contributing to the development of a reliable eye-tracking system for robotic applications.

The machine learning models in this study were implemented using Python 3.10 with the Scikit-learn library. The dataset was split into training and testing subsets with an 80:20 ratio to evaluate the model performance. Specific hyperparameters were used for each algorithm to ensure fair and reproducible comparisons. The decision tree classifier employed the Gini impurity criterion without maximum depth constraints. The support vector machine (SVM) classifier used a radial basis function (RBF) kernel with C = 1.0 and gamma set to 'scale'. The discriminant analysis classifier was performed using the default parameters for linear classification. The Naïve Bayes model used a Gaussian distribution with a smoothing parameter of 1e-9. Meanwhile, the K-nearest neighbors (KNN) algorithm applied Euclidean distance as the metric (p = 2) with k set to 3 and with uniform weights. These configurations were chosen based on common practices in gaze estimation classification tasks and kept consistent across trials. To further ensure model robustness and performance consistency, the experiments were repeated multiple times with randomized data splits, and the average accuracies and inference times were recorded and analyzed.

In addition to the core methodology, several practical challenges were observed during the experiment. Some participants reported mild visual fatigue after multiple gaze fixation cycles, especially during the third replication, which could have influenced the focus and data consistency. This issue was addressed by providing short rest intervals between sessions to maintain participant comfort and data quality. Moreover, intermittent calibration drifts and signal instability occurred, particularly among participants wearing corrective glasses. These disruptions were often caused by glare or reflection from lenses, occasionally affecting the Omron HVC-P camera's ability to track gaze direction precisely. To counteract this, the system was recalibrated in real time whenever signal degradation was detected. While these issues were managed effectively and did not significantly impact the integrity of the dataset, they do represent important considerations for future implementations, especially in more dynamic or less-controlled environments.

III. RESULT

In general, from the three replications carried out, the eye gaze data of the participant ID 1-1 after coordinate processing and cleaning shows that certain targets tended to gather in certain areas. The scatter diagram of the target ID 1-1 shows the consistency of the image capture results from good eye gaze. The presence of the "Null" category, which is indicated by an open circle, indicates unclassified data. This is the boundary used as a sign that the target had moved. The target scatter diagram is shown in Fig. 7.

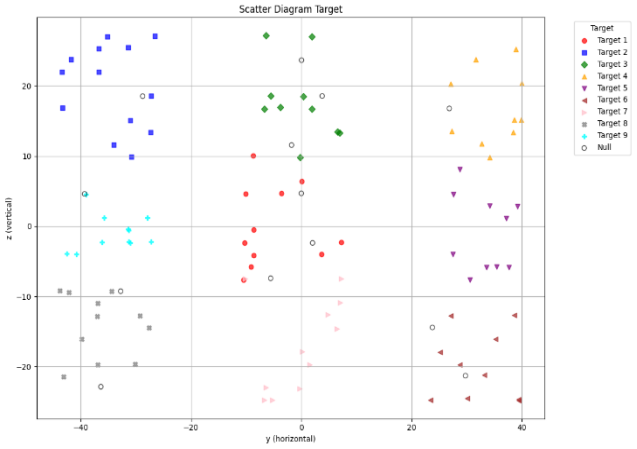

(a)

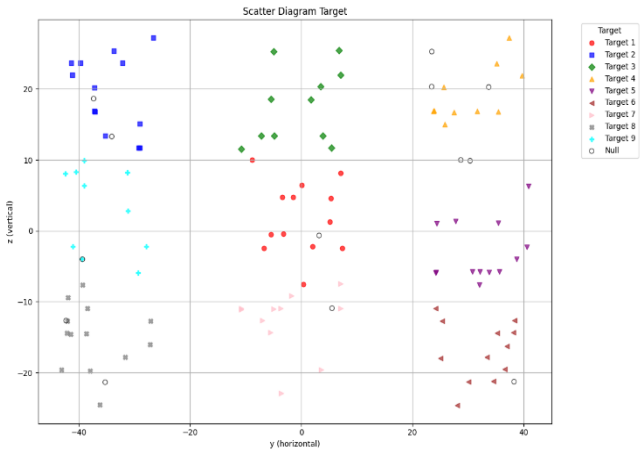

(b)

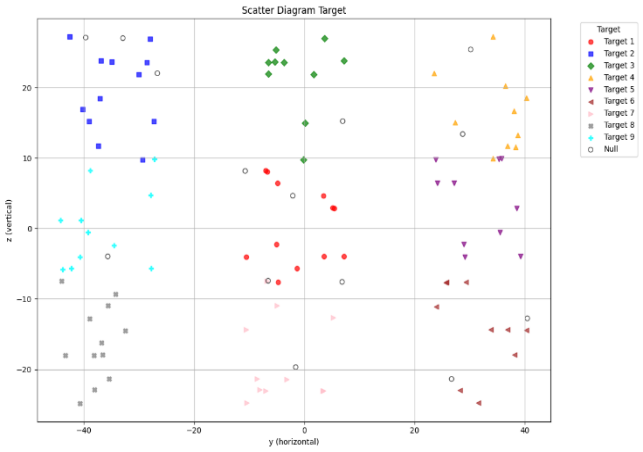

(c)

Fig. 7. Scatter diagram target ID 1-1, (a) replication 1, (b) replication 2, and (c) replication 3

In addition, gaze samples that were labelled as "Null"—defined as gaze points that did not correspond to any of the nine predefined target lockers—were systematically excluded from both training and testing datasets. These Null instances typically arose due to blinks, transient gaze drifts, or brief tracking loss, and were treated as non-informative noise rather than classification errors. The exclusion of such data ensured that only reliable and clearly classified gaze samples were retained for model development and evaluation, minimizing the risk of skewed accuracy metrics.

To ensure the consistency and robustness of the gaze data across multiple replications, we further analyzed the variability of accuracy values within the participants. Specifically, for each machine learning algorithm and participant, we calculated the mean accuracy, standard deviation, and 95% confidence interval across the three replications. This variability analysis provides insights into the reliability of the system over repeated trials. Across all participants and algorithms, the average standard deviation of accuracy was 5.41% (±2.58%), indicating stable performance with relatively low intra-subject variation.

Data from ID 1-1 was then fed into several ML algorithms, producing accuracy as in Table I. The confusion matrix of each ML algorithm for replication 1 of ID 1-1 can be seen in Fig. 8. As shown Fig. 8(a) two testing data points that were wrongly grouped by the decision tree algorithm. The error was that label 1 was interpreted as label 7. This could happen because labels 1 and 7 were adjacent to another. Likewise, label 4 was erroneously interpreted as label 5. Both error patterns were similar. That is to say the correct shelf shifted to the bottom. In Fig. 8(c) the linear discriminant analysis (LDA) algorithm successfully grouped all data correctly because all numbers were diagonal. This shows that there was no misclassification, where each predicted label matched the actual label. This success reflects the effectiveness of the LDA model in distinguishing between different classes of data. With all data correctly classified, this model showed good ability in capturing the characteristics of the features that distinguished each label.

In Fig. 9, the SVM (a), Discriminant Analysis (b), Naïve Bayes (c), and KNN (d) algorithms showed the boundaries of

the prediction data position between shelves. The round dots are the data positions selected as training data, and the square dots are the data positions selected as test data.

The summary of the accuracy of the experimental results for each scenario can be seen in Table II. The study applied a total of eight scenarios, each of which involved three participants, and three replications were carried out for each participant. As a result, a total of 72 replications were produced from various combinations of research participants and scenarios. The data was to be used to test the hypothesized effects eye shape and eyeglass use on machine learning accuracy.

TABLE I. ACCURACY OF SEVERAL ML ALGORITHMS ID 1-1

Algorithms	*Accuracy of replication -*		
	1	*2*	*3*
Decision Tree	90%	82%	90%
Support Vector Machine (SVM)	90%	86%	95%
Discriminant Analysis	100%	86%	95%
Naive Bayes	95%	86%	100%
K-Nearest Neighbors (KNN)	90%	91%	95%

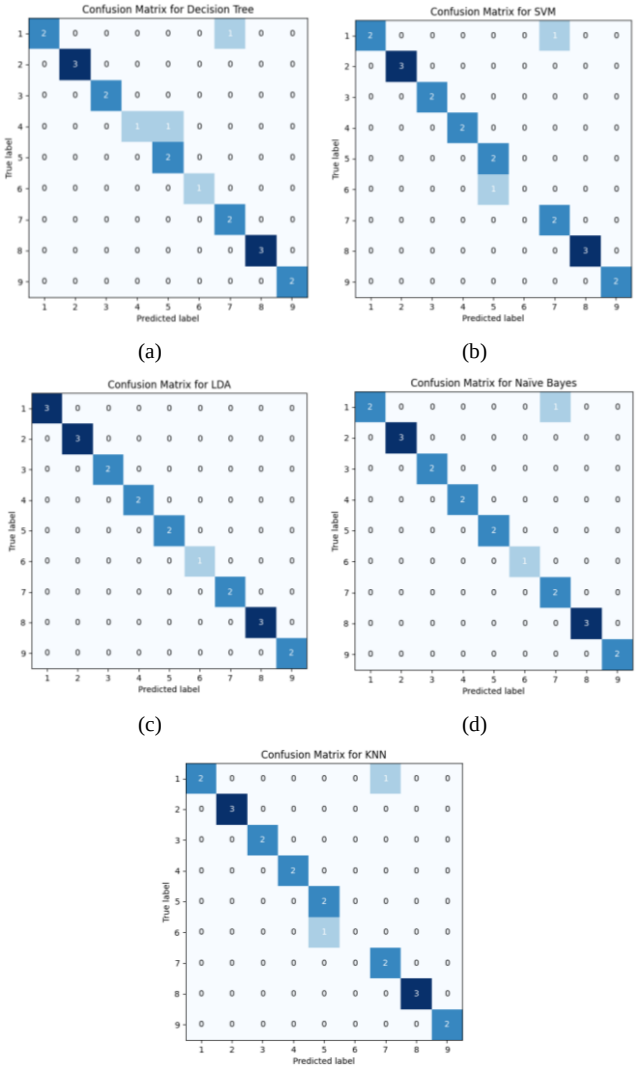

Fig. 8. Confusion matrix for replication 1 ID 1-1, (a) Decision Tree, (b) Support Vector Machine, (c) Discriminant Analysis, (d) Naïve Bayes, and (e) K-Nearest Neighbour

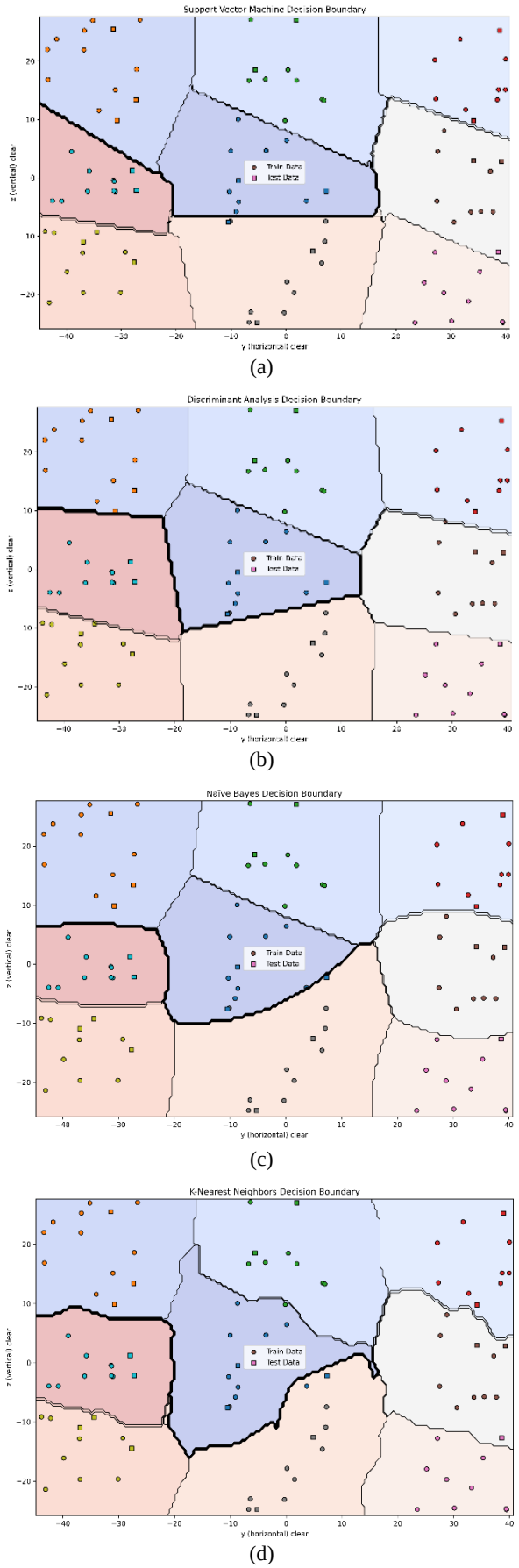

Fig. 9. Visualization of the classification results of each ML algorithm replication 1 ID 1-1, (a) Support Vector Machine, (b) Discriminant Analysis, (c) Naïve Bayes, and (d) K-Nearest Neighbour

TABLE II. ACCURACY OF SEVERAL ML ALGORITHMS

No.	ID	Rep	DT	SVM	LDA	NB	KNN
1	1-1	1	0.900	0.900	1.000	0.950	0.900
2	1-1	2	0.818	0.864	0.864	0.864	0.909
3	1-1	3	0.900	0.950	0.950	1.000	0.950
4	1-2	1	0.952	0.905	0.857	0.952	0.857
5	1-2	2	0.750	0.950	0.950	0.800	0.800
6	1-2	3	0.952	0.905	0.905	0.905	0.857
7	1-3	1	1.000	0.955	0.955	0.864	0.773
8	1-3	2	1.000	1.000	1.000	0.952	1.000
9	1-3	3	0.952	0.952	1.000	1.000	1.000
10	2-1	1	0.905	0.857	0.857	0.952	0.810
11	2-1	2	0.864	0.818	0.909	0.909	0.909
12	2-1	3	1.000	0.864	0.955	0.864	0.909
13	2-2	1	0.952	1.000	1.000	1.000	1.000
14	2-2	2	1.000	0.857	0.905	0.905	0.905
15	2-2	3	0.857	0.857	0.857	0.905	0.905
16	2-3	1	0.857	0.810	0.810	0.762	0.810
17	2-3	2	0.952	0.952	0.952	0.952	0.952
18	2-3	3	0.905	0.905	0.857	0.810	0.905
19	3-1	1	0.952	0.857	0.952	0.905	0.857
20	3-1	2	0.810	0.762	0.905	1.000	0.857
21	3-1	3	0.818	0.909	0.864	0.909	0.909
22	3-2	1	0.955	0.955	0.955	0.955	0.909
23	3-2	2	0.952	0.905	0.857	0.952	0.952
24	3-2	3	0.905	0.952	0.952	0.952	1.000
25	3-3	1	0.905	0.905	0.905	0.905	0.857
26	3-3	2	0.864	0.909	0.909	0.864	0.909
27	3-3	3	1.000	0.955	1.000	1.000	0.955
28	4-1	1	0.857	0.857	0.857	0.810	0.857
29	4-1	2	0.905	0.857	0.905	0.762	0.810
30	4-1	3	0.857	0.857	0.857	0.905	0.905
31	4-2	1	1.000	1.000	1.000	1.000	1.000
32	4-2	2	0.952	0.952	1.000	0.952	1.000
33	4-2	3	0.909	0.955	0.955	0.909	0.864
34	4-3	1	0.905	0.857	0.857	0.952	0.857
35	4-3	2	0.952	0.905	0.952	0.952	0.952
36	4-3	3	0.952	0.952	0.952	0.905	0.905
37	5-1	1	0.955	0.955	0.955	1.000	0.864
38	5-1	2	0.857	0.810	0.857	0.810	0.810
39	5-1	3	0.955	0.955	0.955	0.955	0.864
40	5-2	1	0.905	1.000	1.000	1.000	1.000
41	5-2	2	0.950	0.950	0.900	0.900	0.950
42	5-2	3	1.000	0.909	0.955	0.864	0.909
43	5-3	1	0.952	1.000	0.952	1.000	1.000
44	5-3	2	0.955	0.909	0.864	0.864	0.864
45	5-3	3	0.905	0.905	0.952	0.905	0.905
46	6-1	1	0.952	0.857	0.905	0.857	0.952
47	6-1	2	0.952	0.857	1.000	0.905	0.952
48	6-1	3	0.952	1.000	0.857	0.810	0.905
49	6-2	1	0.900	0.850	0.900	0.850	0.850
50	6-2	2	0.850	0.800	0.850	0.850	0.900
51	6-2	3	0.955	0.909	0.864	0.909	0.818
52	6-3	1	0.909	0.909	0.864	0.864	0.864
53	6-3	2	1.000	1.000	1.000	1.000	0.952
54	6-3	3	0.905	0.905	1.000	0.952	1.000
55	7-1	1	1.000	0.955	1.000	0.955	0.955
56	7-1	2	1.000	0.952	0.857	0.952	0.810
57	7-1	3	0.952	0.905	0.952	0.905	0.857
58	7-2	1	0.905	0.952	0.952	0.952	0.952
59	7-2	2	1.000	0.955	0.955	1.000	0.909
60	7-2	3	0.905	0.905	0.952	0.905	0.857
61	7-3	1	0.900	0.850	0.950	0.750	0.800
62	7-3	2	1.000	0.857	0.952	0.857	0.810
63	7-3	3	0.950	0.950	0.900	0.900	0.850
64	8-1	1	0.857	0.810	0.810	0.762	0.810
65	8-1	2	0.909	0.818	0.818	0.864	0.909
66	8-1	3	0.952	0.857	0.905	0.857	0.857
67	8-2	1	0.955	0.955	0.955	0.955	0.955
68	8-2	2	1.000	0.952	0.952	0.952	0.905
69	8-2	3	0.857	0.905	0.857	0.905	0.905
70	8-3	1	0.857	0.952	0.857	0.810	0.810
71	8-3	2	0.810	0.714	0.857	0.810	0.762
72	8-3	3	1.000	0.900	0.950	0.900	0.900

IV. DISCUSSION

Statistical testing was conducted to determine the relationship between eye shape and the accuracy of each machine learning (ML) model. This was done to obtain a fair comparison and increase confidence in the conclusions of the tests conducted. Eye shapes were categorized into two groups: monolid and non-monolid. The monolid shape used data from participants in scenarios 3, 4, 7, and 8. The non-monolid shape used data from participants in scenarios 1, 2, 5, and 6.

An ANOVA test was performed on the monolid and non-monolid eye shapes regarding the accuracy of the ML Decision Tree algorithm with the following hypotheses:

Null hypothesis : All means are equal

Alternative hypothesis : Not all means are equal

Significance level : $\alpha = 0.05$

As shown in Table III, the p-value was significantly above the significance level, leading to the decision not to reject the null hypothesis. The conclusion of this test demonstrates that the average accuracy values of the Decision Tree ML algorithm for the monolid and non-monolid eye shapes were the same. However, the non-monolid eye shape had a higher average accuracy compared to the monolid eye shape.

TABLE III. ANALYSIS OF VARIANCE OF EYE SHAPE ACCURACY AGAINST THE DECISION TREE ML ALGORITHM

Source	DF	Adj SS	Adj MS	F-Value	P-Value
Eye shape	1	0.000062	0.000062	0.02	0.893
Error	70	0.235040	0.003358		
Total	71	0.235102			

The accuracy values with a 95% confidence interval can be seen in Fig. 10(a). Although the non-monolid eye shape had a higher average accuracy than did the monolid eye shape, individually, the accuracy values for the monolid eye shape reached 100% a total of eight times, compared to the six times reached by the non-monolid eye shape. The individual value plot is shown in Fig. 10(b), and the box plot is presented in Fig. 10(c).

Employing the same hypothesis testing procedure as utilized for the Decision Tree algorithm, the ANOVA results achieved for other machine learning algorithms are presented in Table IV. As indicated in Table IV, the p-value was considerably higher than the significance level, resulting in the conclusion not to reject the null hypothesis. This test concluded that the average accuracy values of the Support Vector Machine, Discriminant Analysis, Naïve Bayes, and K-Nearest Neighbors algorithms concerning the monolid and non-monolid eye shapes were equivalent.

For the support vector machine (SVM) algorithm, although the ANOVA results do not reveal any significant difference in average accuracy, the non-monolid eye shape had a higher average accuracy compared to the monolid eye shape. The accuracy values with a 95% confidence interval can be seen in Fig. 11(a). The non-monolid eye shape achieved a higher average accuracy than the monolid eye shape. Individually, the accuracy value for the monolid eye

shape reached 100% only once, while the non-monolid eye shape achieved 100% a total of six times. The Individual Value Plot is shown in Fig. 11(b), and the box plot is presented in Fig. 11(c).

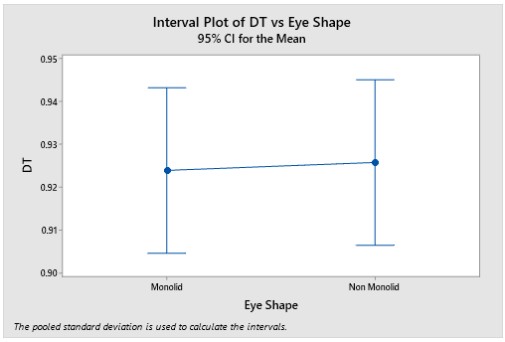

(a)

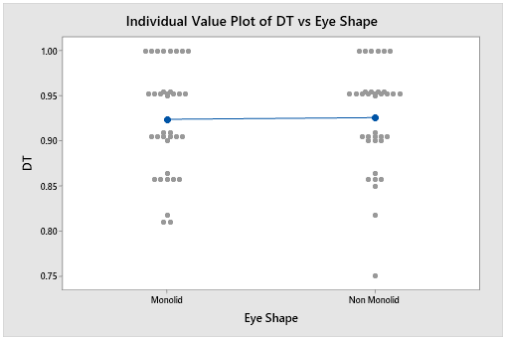

(b)

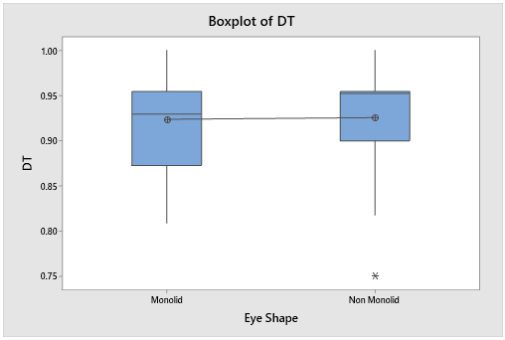

(c)

Fig. 10. (a) Interval plot 95% CI of decision tree vs eye shape, (b) Individual value plot of decision tree vs eye shape, and (c) boxplot of decision tree

TABLE IV. ANALYSIS OF VARIANCE OF EYE SHAPE ACCURACY AGAINST THE SVM, DA, NB AND KNN ML ALGORITHM

Source	DF	Adj SS	Adj MS	F-Value	P-Value
Support Vector Machine (SVM)					
Eye shape	1	0.000062	0.000062	0.02	0.893
Error	70	0.235040	0.003358		
Total	71	0.235102			
Discriminant Analysis (DA)					
Eye shape	1	0.000062	0.000062	0.02	0.893
Error	70	0.235040	0.003358		
Total	71	0.235102			
Naïve Bayes (NB)					
Eye shape	1	0.000062	0.000062	0.02	0.893
Error	70	0.235040	0.003358		
Total	71	0.235102			
K-Nearest Neighbor (KNN)					
Eye shape	1	0.000062	0.000062	0.02	0.893
Error	70	0.235040	0.003358		
Total	71	0.235102			

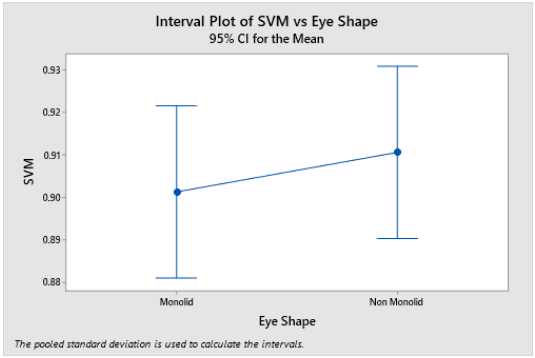

(a)

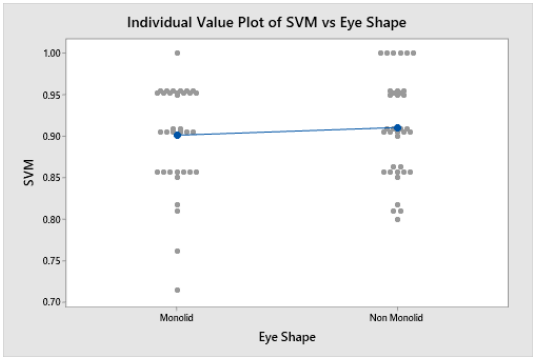

(b)

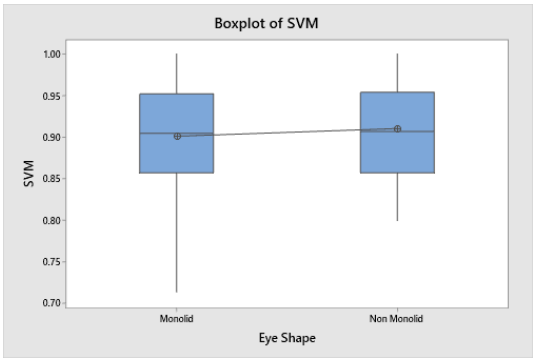

(c)

Fig. 11. (a) Interval plot 95% CI of SVM vs eye shape, (b) Individual value plot of SVM vs eye shape, and (c) Boxplot of SVM

For the discriminant analysis (LDA) algorithm, although the ANOVA results do not reveal any significant difference in average accuracy, the non-monolid eye shape has a higher average accuracy compared to the monolid eye shape. The accuracy values with a 95% confidence interval can be seen in Fig. 12(a). The non-monolid eye shape achieved a higher average accuracy than the monolid eye shape. Individually, the accuracy value for the monolid eye shape reached 100% only four times, while the non-monolid eye shape achieved 100% a total of eight times. The individual value plot is shown in Fig. 12(b), and the box plot is presented in Fig. 12(c).

For the naïve bayes (NB) algorithm, although the ANOVA results do not reveal any significant difference in average accuracy, the non-monolid eye shape had a higher average accuracy compared to the monolid eye shape. The accuracy values with a 95% confidence interval can be seen in Fig. 13(a). The non-monolid eye shape achieved a higher

average accuracy than the monolid eye shape. Individually, the accuracy value for the monolid eye shape reached 100% only four times, while the non-monolid eye shape achieved 100% a total of eight times. The individual value plot is shown in Fig. 13(b), and the box plot is presented in Fig. 13(c).

For the K-Nearest Neighbors (KNN) algorithm, although the ANOVA results do not reveal any significant difference in average accuracy, the non-monolid eye shape hax a higher average accuracy compared to the monolid eye shape. The accuracy values with a 95% confidence interval can be seen in Fig. 14(a). The non-monolid eye shape achieved a higher average accuracy than the monolid eye shape. Individually, the accuracy value for the monolid eye shape reached 100% only three times, while the non-monolid eye shape achieved 100% a total of six times. The Individual Value Plot is shown in Fig. 14(b), and the Box Plot is presented in Fig. 14(c).

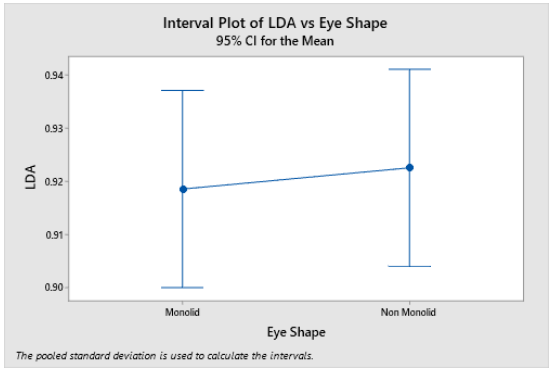

(a)

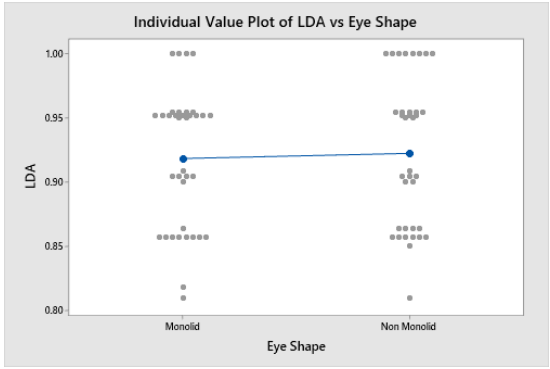

(b)

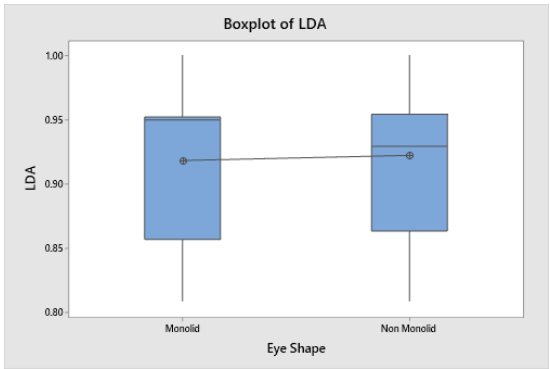

(c)

Fig. 12. (a) Interval plot 95% CI of LDA vs eye shape, (b) Individual value plot of LDA vs eye shape, and (c) Boxplot of LDA

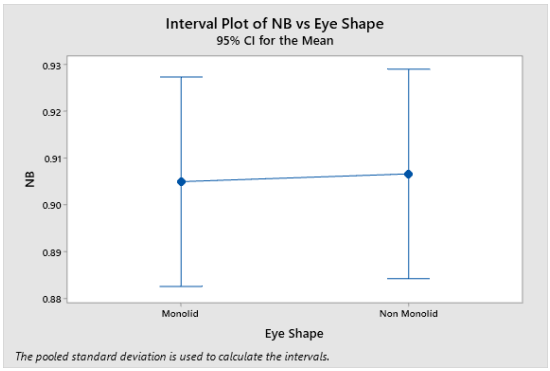

(a)

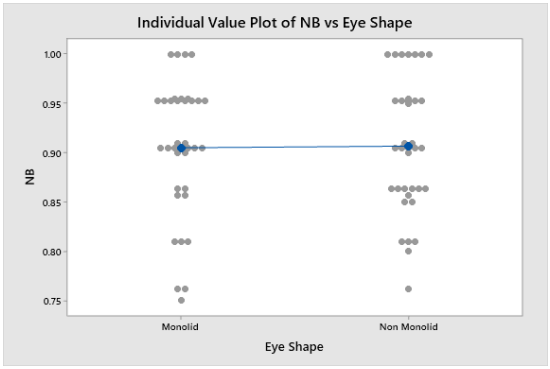

(b)

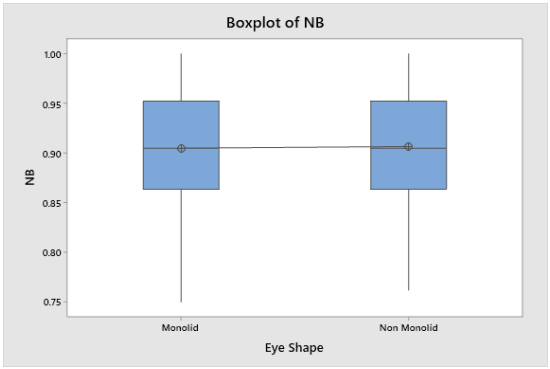

(c)

Fig. 13. (a) Interval plot 95% CI of NB vs eye shape, (b) Individual value plot of NB vs eye shape, and (c) Boxplot of NB

Based on the statistical testing of each machine learning algorithm against the monolid and non-monolid eye shapes, the accuracy of the developed system was uniform for each eye shape. This indicates that the system could be applied to individuals with both monolid and non-monolid eye shapes without any significant changes in accuracy.

Although there were no statistically significant differences in average accuracy, the data indicates that the average accuracy produced by participants with non-monolid eye shapes was higher than that produced by those with monolid eye shapes. This superior accuracy was observed across all the five machine learning algorithms used, leading to the conclusion that, on average, the non-monolid eye shape was definitively better than the monolid eye shape.

Next, we specifically tested the relationship between the use of glasses among research participants and the accuracy values. The testing was conducted for each machine learning

algorithm. This was done to obtain a fair comparison and to enhance confidence in the conclusions drawn from the tests.

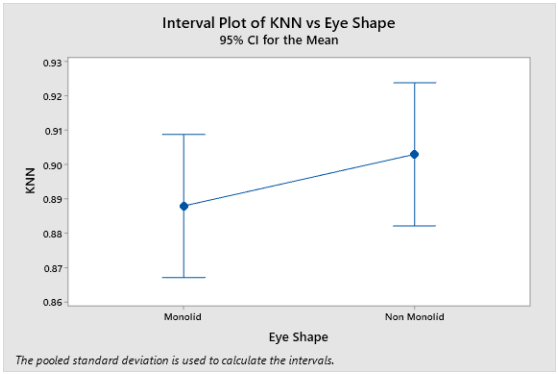

(a)

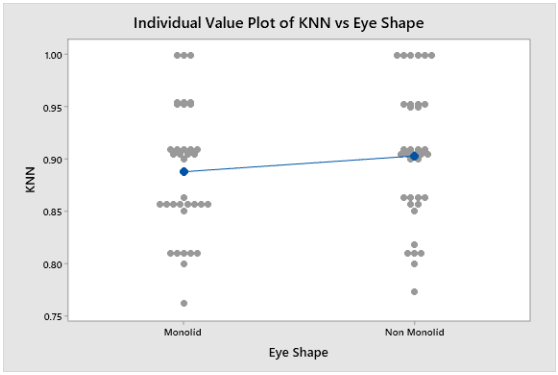

(b)

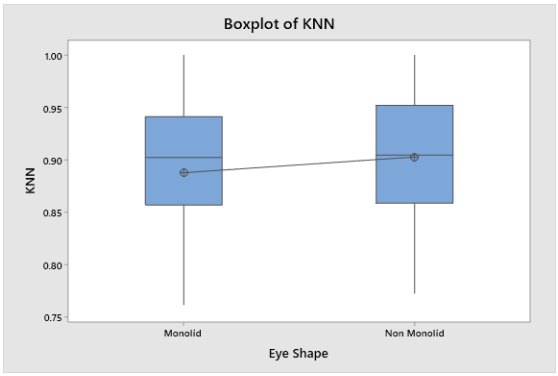

(c)

Fig. 14. (a) Interval plot 95% CI of KNN vs eye shape, (b) Individual value plot of KNN vs eye shape, and (c) Boxplot of KNN

Statistical testing was conducted to determine the relationship between glasses use and the accuracy of each machine learning (ML) model. Glasses use was categorized into two groups: glasses wearing and glasses non-wearing. The glasses wearing criteria used data from participants in scenarios 5, 6, 7, and 8. Meanwhile, the glasses non-wearing criteria used data from participants in scenarios 1, 2, 3, and 4. An ANOVA test was performed on the glasses and non-glasses regarding the accuracy of the All-ML algorithm with the following hypotheses:

Null hypothesis : All means are equal

Alternative hypothesis : Not all means are equal

Significance level : $\alpha = 0.05$

The ANOVA test results for other machine learning algorithms are presented in Table V.

TABLE V. ANALYSIS OF VARIANCE OF GLASSES USED ACCURACY AGAINST THE DT, SVM, DA, NB AND KNN ML ALGORITHM

Source	DF	Adj SS	Adj MS	F-Value	P-Value
Decision Tree (DT)					
Eye shape	1	0.005856	0.005856	1.79	0.185
Error	70	0.229246	0.003275		
Total	71	0.235102			
Support Vector Machine (SVM)					
Eye shape	1	0.000007	0.000007	0.00	0.967
Error	70	0.260912	0.003727		
Total	71	0.260918			
Discriminant Analysis (DA)					
Eye shape	1	0.000336	0.000336	0.11	0.743
Error	70	0.217307	0.003104		
Total	71	0.217643			
Naïve Bayes (NB)					
Eye shape	1	0.005903	0.005903	1.32	0.254
Error	70	0.312281	0.004461		
Total	71	0.318184			
K-Nearest Neighbor (KNN)					
Eye shape	1	0.003996	0.003996	1.01	0.318
Error	70	0.276034	0.003943		
Total	71	0.280029			

Employing the same hypothesis testing procedure as utilized for eye shape, the ANOVA results achieved for all machine learning algorithms (glasses use) are presented in Table V. The data in Table V indicates that the p-value was considerably higher than the significance level, resulting in the conclusion not to reject the null hypothesis. This test concluded that the average accuracy values of the decision tree, support vector machine, discriminant analysis, naïve bayes, and K-nearest neighbors algorithms concerning the use of glasses were equivalent.

The statistical analyses using ANOVA indicate no significant differences in gaze estimation accuracy between groups based on eye shape (monolid vs. non-monolid) and glasses use (glasses wearing vs. glasses non-wearing) across all the five machine learning algorithms. While these results support the robustness and generalizability of the developed system, it is important to acknowledge the methodological assumptions and practical implications associated with these analyses.

ANOVA relies on assumptions of normality of residuals and homogeneity of variances. Although the number of participants per group was modest (n = 12), each participant contributed a substantial number of gaze samples (324 data points per participant, derived from nine target positions × 12 samples per target × three replications), resulting in a total dataset size that was sufficiently large for robust statistical analysis and model training. Furthermore, the balanced design across groups (equal distribution of eye shape and glasses status) helped to mitigate potential violations of these assumptions. Prior literature suggests that ANOVA remains robust to moderate deviations from normality and variance homogeneity under such conditions.

Beyond statistical significance, it is also valuable to consider the practical significance of observed trends in the data. Although no statistically significant differences were detected, participants with a non-monolid eye shape consistently achieved a higher average accuracy across all five algorithms compared to those with monolid eyes. Similarly, participants without glasses generally exhibited marginally higher performance than glasses-wearers, particularly when using the Naïve Bayes and K-Nearest Neighbors (KNN) algorithms. These patterns, while not conclusive, highlight potential areas for further investigation and system refinement.

The lower average accuracy observed for glasses-wearers when using Naïve Bayes and KNN models may be attributable to the inherent sensitivities of these algorithms. The Naïve Bayes model assumes feature independence and may be adversely affected by the non-linear distortions introduced by eyeglass lenses, such as refraction artifacts or specular reflections. Meanwhile, the KNN model relies on local neighborhood density for classification, which can be disrupted by small positional shifts or the inconsistencies caused by lens reflections and calibration noise. These factors may have introduced additional variability in gaze feature distributions, reducing model performance.

Potential confounding factors, such as lighting reflections, lens distortions, and calibration drifts, were systematically controlled in our experimental design. All experiments were conducted under standardized lighting conditions (an average of 429 lux with minimal variability), and a nine-point calibration was performed for each participant prior to data collection. The use of a fixed camera position and a static head pose further minimized extraneous variability. Nevertheless, we recognized that residual effects of these factors—particularly subtle reflections and minor misalignments in glasses-wearers—may have contributed to the observed trends and warrant further exploration in future studies.

These findings suggest that while the developed gaze-based control system demonstrated statistically consistent performance across diverse user characteristics, continued refinement to enhance robustness against anatomical and optical variability is warranted, especially for users wearing corrective eyewear.

Our findings complement and extend prior research in gaze estimation [41]–[71] by demonstrating that spatial control accuracy remained consistent across eye shape and eyewear groups when evaluated using multiple machine learning classifiers under controlled conditions. Previous studies have primarily focused on enhancing robustness under dynamic lighting or head pose conditions [52]–[56] and explored applications in assistive and collaborative robotics [12]–[14], [57]–[59], yet few have systematically assessed how anatomical differences influence classifier performance. For example, [63]–[66] noted reduced scleral visibility in participants with monolid eyes as a challenge for gaze detection, and [67]–[71] reported accuracy issues due to lens reflections in glasses-wearers. Unlike these studies, our results show no statistically significant difference in accuracy across these user traits, indicating the feasibility of an inclusive system. The contribution of this research takes the form of a structured, multi-classifier evaluation that isolates human anatomical factors—eye shape and eyewear—as experimental variables, thereby validating the robustness of traditional ML methods for inclusive, real-time robot control. This provides a new benchmark for designing accessible human-robot interaction systems.

If we look at the average accuracy for each ML algorithm, there were interesting observations to note. The ML Decision Tree classifier showed that using glasses would improve the average accuracy. As seen in Fig. 15(a), there was a noticeable difference in the average accuracy between participants who wore glasses and those who did not. The ML SVM classifier indicated that the accuracy was relatively the same whether glasses were used or not, as shown in Fig. 15(b). This was also reflected in the p-value of the ML SVM classifier, which was 0.967 (almost equal to 1). Meanwhile, the ML Naïve Bayes, KNN, and LDA algorithms showed that the average accuracy for those using glasses was lower than for those not using glasses. As seen in Figs. 15(c), 15(d), and 15(e), there was a noticeable difference in the average accuracy between participants who wore glasses and those who did not.

Although the statistical analyses did not reveal significant differences in accuracy between participants with different eye shapes or eyewear statuses, subtle trends were consistently observed across all machine learning models. Specifically, participants with non-monolid eyes and non-glasses wearers tended to achieve a marginally higher accuracy on average. One possible explanation for this trend is that non-monolid eyes generally exhibit greater scleral exposure, which can enhance contrast and visibility of the eye features used in gaze estimation. This facilitates more accurate feature detection and reduces ambiguity in coordinate mapping. Similarly, participants without glasses may have experienced fewer optical artifacts, such as lens reflections or light distortions, which are known to interfere with infrared- or image-based gaze tracking systems. These factors, while not strong enough to produce statistically significant effects in this study, may nevertheless influence real-world system robustness.

The practical implications of these findings suggest that gaze-based control systems should account for subtle variations in user anatomy and eyewear status to maximize inclusiveness. Adaptive calibration methods or model fine-tuning based on user profiles may enhance performance across diverse populations. Furthermore, the fact that non-monolid and glasses-wearing participants still achieved comparable performance despite these potential limitations supports the feasibility of deploying a single unified system across user groups, with minimal performance degradation.

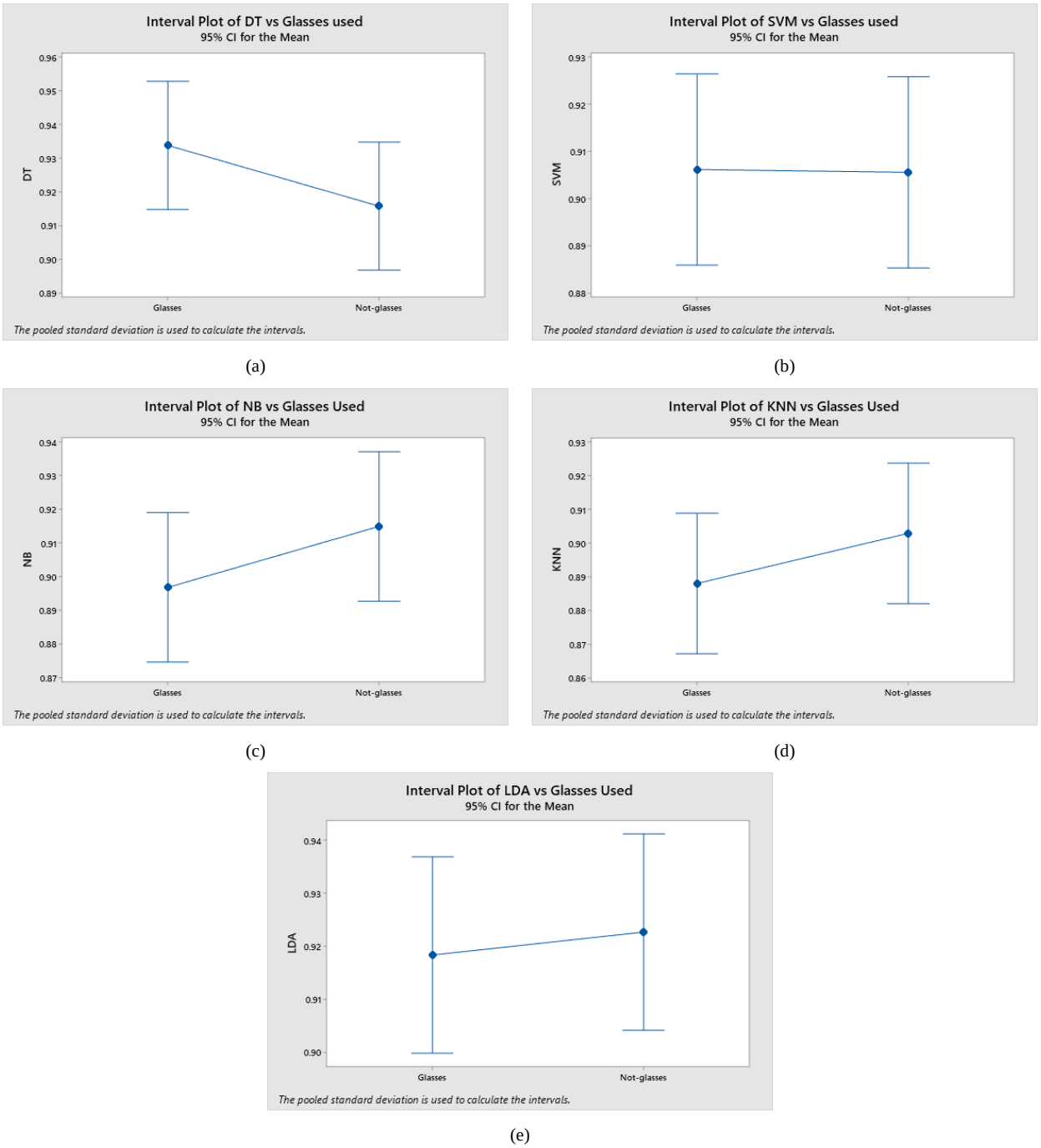

Fig. 15. 95% Confidence interval plot (a) of Decision Tree vs. glasses use, (b) SVM vs. glasses use, (c) Naïve Bayes vs. glasses use, (d) KNN vs. glasses use, and (e) Discriminant Analysis vs. glasses used

This study offers several strengths that support the validity of the findings. The experimental protocol was carefully designed with controlled lighting conditions (~429 lux), standardized calibration procedures, and repeated trials to ensure consistency and minimize confounding variables. The use of five different machine learning algorithms provided a comprehensive evaluation of classifier behavior under the influence of varying user characteristics. However, the study also has limitations. The experiment was conducted in a static and controlled indoor environment, which did not fully reflect real-world conditions where lighting variation, head movements, and background noise can influence system performance.

To extend the applicability of this work, future studies may investigate additional anatomical features, such as pupil size, eyelid curvature, or eye openness. Environmental factors, including ambient lighting conditions and dynamic head movements, should also be examined to assess their impact on system accuracy and usability. Incorporating multimodal data—such as head pose or blink frequency—may further improve system adaptability, enabling more robust human-robot interactions in uncontrolled settings.

V. CONCLUSION

This study has investigated the impact of eye shape and glasses use on the accuracy of robot control via eye-gaze

technology. The findings indicate that, despite minor variations, the accuracy of gaze-based control remains statistically consistent across different eye morphologies and irrespective of the presence or absence of glasses. However, it is important to acknowledge certain limitations and practical trends observed in the study.

Although statistical analyses revealed no significant differences, participants with a non-monolid eye shape consistently achieved a marginally higher average accuracy across all five machine learning algorithms compared to those with monolid eyes. Similarly, glasses-wearers exhibited a slightly lower average accuracy, particularly when using naïve bayes and K-nearest neighbors algorithms. These trends, while not statistically conclusive, suggest potential areas for further refinement and optimization of gaze-based systems.

Potential confounding factors, such as lighting reflections, lens distortions, and calibration drifts, were carefully controlled through standardized illumination, consistent calibration procedures, and fixed experimental geometry. Nevertheless, the residual effects of these factors may have subtly influenced the results and should be considered in future investigations.

These findings contribute to the development of more inclusive and universally applicable eye-gaze-based robotic control systems. By confirming that existing eye-tracking and machine learning models can perform consistently across diverse user characteristics, this research underscores the viability of gaze-based control systems in real-world applications, particularly for individuals with physical disabilities or those requiring hands-free robotic interactions.

While the study demonstrates the robustness of gaze-based robot control systems across diverse eye shapes and eyewear conditions, it is important to acknowledge certain limitations. The experiment was conducted in a controlled indoor setting with stable lighting and under static head pose constraints. These controlled conditions, while valuable for isolating key variables, may not fully reflect the complexity of real-world environments. Therefore, care should be taken when generalizing the findings beyond the scope of the present study.

Despite these limitations, the results highlight the significant societal value of inclusive gaze-based control systems. In the realm of assistive technologies, such systems offer a non-invasive and accessible means of interaction for individuals with motor impairments, potentially enhancing autonomy and quality of life. In industrial and collaborative robotics, the ability to accommodate diverse anatomical features and visual aids wearing supports broader workforce integration and safer human-robot cooperation. These insights reaffirm the importance of designing adaptive and inclusive human-machine interfaces in alignment with Industry 5.0 principles.

A promising direction for future research is the incorporation of dynamic head pose estimation, which can improve robustness and user experience by allowing natural head movements. However, it is important to recognize that implementing dynamic head pose tracking introduces additional challenges, including increased computational complexity, higher real-time processing demands, and the need for algorithms that can compensate for motion-related artifacts. In addition to head pose integration, further research should explore enhancements of algorithm adaptability to individual anatomical differences, such as variations in eye morphology and eyelid structure, and improvements of system robustness under diverse environmental conditions, including lighting variability and potential sensor occlusions. Addressing these challenges will contribute to the development of more accurate, adaptable, and user-friendly gaze-based robotic control systems suitable for practical deployment in dynamic and heterogeneous user environments.

REFERENCES

[1] G. Daemmer, S. Gablenz, R. Neumann, and Z. Major, "Design, topology optimization, and additive manufacturing of a pneumatically actuated lightweight robot," *Actuators*, vol. 12, no. 7, p. 266, 2023, doi: 10.3390/act12070266.

[2] Z. Li and S. Li, "Time-optimal constrained kinematic control of robotic manipulators by recurrent neural network," *Expert Systems with Applications*, vol. 257, p. 124994, 2024, doi: 10.1016/j.eswa.2024.124994.

[3] J. Qu, Z. Yu, W. Tang, Y. Xu, B. Mao, and K. Zhou, "Advanced technologies and applications of robotic soft grippers," *Advanced Materials Technologies*, vol. 9, no. 11, p. 2301004, 2024, doi: 10.1002/admt.202301004.

[4] A. J. Fuge, C. W. Herron, B. C. Beiter, B. Kalita, and A. Leonessa, "Design, development, and analysis of the lower body of next-generation 3D-printed humanoid research platform: PANDORA," *Robotica*, vol. 41, no. 7, pp. 2177–2206, Jul. 2023, doi: 10.1017/S0263574723000395.

[5] S. J. Oh, "Emergence of a new sector via a business ecosystem: a case study of Universal Robots and the collaborative robotics sector," *Technology Analysis and Strategic Management*, vol. 35, no. 6, pp. 645–658, 2023, doi: 10.1080/09537325.2021.1986212.

[6] M. Soori, R. Dastres, B. Arezoo, and F. K. G. Jough, "Intelligent robotic systems in Industry 4.0: A review," *Journal of Advanced Manufacturing Science and Technology*, vol. 4, no. 3, 2024, doi: 10.51393/j.jamst.2024007.

[7] J. Iqbal, Z. H. Khan, and A. Khalid, "Prospects of robotics in food industry," *Food Science and Technology (Brazil)*, vol. 37, no. 2, pp. 159–165, 2017, doi: 10.1590/1678-457X.14616.

[8] M. Javaid, A. Haleem, R. P. Singh, and R. Suman, "Substantial capabilities of robotics in enhancing industry 4.0 implementation," *Cognitive Robotics*, vol. 1, pp. 58–75, 2021, doi: 10.1016/j.cogr.2021.06.001.

[9] T. T. Thuong and V. T. Ha, "Adaptive Control For Mobile Robots Based On Inteligent Controller," *Journal of Applied Science and Engineering*, vol. 27, no. 5, pp. 2481–2487, 2023, doi: 10.6180/jase.202405_27(05).0012.

[10] M. Choe, Y. Choi, J. Park, and J. Kim, "Head Mounted IMU-Based Driver's Gaze Zone Estimation Using Machine Learning Algorithm," *International Journal of Human–Computer Interaction*, vol. 40, no. 23, pp. 7970–7981, Dec. 2024, doi: 10.1080/10447318.2023.2276520.

[11] F. B. Narcizo, F. E. D. dos Santos, and D. W. Hansen, "High-Accuracy Gaze Estimation for Interpolation-Based Eye-Tracking Methods," *Vision*, vol. 5, no. 3, p. 41, Sep. 2021, doi: 10.3390/vision5030041.

[12] J. Guo *et al.*, "A Novel Robotic Guidance System With Eye-Gaze Tracking Control for Needle-Based Interventions," *IEEE Transactions on Cognitive and Developmental Systems*, vol. 13, no. 1, pp. 179–188, Mar. 2021, doi: 10.1109/TCDS.2019.2959071.

[13] L. Wöhle and M. Gebhard, "Towards Robust Robot Control in Cartesian Space Using an Infrastructureless Head- and Eye-Gaze Interface," *Sensors*, vol. 21, no. 5, p. 1798, Mar. 2021, doi: 10.3390/s21051798.

[14] J. Meyer, S. Gering, and E. Kasneci, "Static Laser Feedback Interferometry-Based Gaze Estimation for Wearable Glasses," *IEEE*

Sensors Journal, vol. 23, no. 7, pp. 7558–7569, Apr. 2023, doi: 10.1109/JSEN.2023.3250714.

[15] F. Kano, Y. Kawaguchi, and Y. Hanling, "Experimental evidence that uniformly white sclera enhances the visibility of eye-gaze direction in humans and chimpanzees," *eLife*, vol. 11, Mar. 2022, doi: 10.7554/eLife.74086.

[16] J. Xu, Z. Huang, L. Liu, X. Li, and K. Wei, "Eye-Gaze Controlled Wheelchair Based on Deep Learning," *Sensors*, vol. 23, no. 13, p. 6239, Jul. 2023, doi: 10.3390/s23136239.

[17] V. Krishna Sharma, K. Saluja, V. Mollyn, and P. Biswas, "Eye Gaze Controlled Robotic Arm for Persons with Severe Speech and Motor Impairment," in *ACM Symposium on Eye Tracking Research and Applications*, pp. 1–9, Jun. 2020, doi: 10.1145/3379155.3391324.

[18] D. Cojocaru, L. F. Manta, I. C. Vladu, A. Dragomir, and A. M. Mariniuc, "Using an Eye Gaze New Combined Approach to Control a Wheelchair Movement," in *2019 23rd International Conference on System Theory, Control and Computing (ICSTCC)*, pp. 626–631, Oct. 2019, doi: 10.1109/ICSTCC.2019.8886158.

[19] S. Ban, Y. J. Lee, K. J. Yu, J. W. Chang, J.-H. Kim, and W.-H. Yeo, "Persistent Human–Machine Interfaces for Robotic Arm Control Via Gaze and Eye Direction Tracking," *Advanced Intelligent Systems*, vol. 5, no. 7, Jul. 2023, doi: 10.1002/aisy.202200408.

[20] L. Maule *et al.*, "RoboEye, an Efficient, Reliable and Safe Semi-Autonomous Gaze Driven Wheelchair for Domestic Use," *Technologies*, vol. 9, no. 1, p. 16, Feb. 2021, doi: 10.3390/technologies9010016.

[21] L. Wang and S. Li, "Wheelchair-Centered Omnidirectional Gaze-Point Estimation in the Wild," *IEEE Transactions on Human-Machine Systems*, vol. 53, no. 3, pp. 466–478, Jun. 2023, doi: 10.1109/THMS.2023.3263541.

[22] X. Zhang *et al.*, "Design and Evaluation of the Extended FBS Model Based Gaze-Control Power Wheelchair for Individuals Facing Manual Control Challenges," *Sensors*, vol. 23, no. 12, p. 5571, Jun. 2023, doi: 10.3390/s23125571.

[23] I. Svensson *et al.*, "Effects of assistive technology for students with reading and writing disabilities," *Disability and Rehabilitation: Assistive Technology*, vol. 16, no. 2, pp. 196–208, Feb. 2021, doi: 10.1080/17483107.2019.1646821.

[24] J. M. Fernández-Batanero, M. Montenegro-Rueda, J. Fernández-Cerero, and I. García-Martínez, "Assistive technology for the inclusion of students with disabilities: a systematic review," *Educational technology research and development*, vol. 70, no. 5, pp. 1911–1930, Oct. 2022, doi: 10.1007/s11423-022-10127-7.

[25] G. Yenduri *et al.*, "From Assistive Technologies to Metaverse—Technologies in Inclusive Higher Education for Students With Specific Learning Difficulties: A Review," *IEEE Access*, vol. 11, pp. 64907–64927, 2023, doi: 10.1109/ACCESS.2023.3289496.

[26] X.-F. Yuan, Y.-Q. Ji, T.-X. Zhang, H.-B. Xiang, Z.-Y. Ye, and Q. Ye, "Effects of Exercise Habits and Gender on Sports e-Learning Behavior: Evidence from an Eye-Tracking Study," *Psychology Research and Behavior Management*, vol. 17, pp. 813–826, Feb. 2024, doi: 10.2147/PRBM.S442863.

[27] P. W. Laksono *et al.*, "Mapping Three Electromyography Signals Generated by Human Elbow and Shoulder Movements to Two Degree of Freedom Upper-Limb Robot Control," *Robotics*, vol. 9, no. 4, p. 83, Oct. 2020, doi: 10.3390/robotics9040083.

[28] X. Wang and V. J. Santos, "Gaze-Based Shared Autonomy Framework With Real-Time Action Primitive Recognition for Robot Manipulators," *IEEE Transactions on Neural Systems and Rehabilitation Engineering*, vol. 31, pp. 4306–4317, 2023, doi: 10.1109/TNSRE.2023.3328888.

[29] A. Fischer-Janzen, T. M. Wendt, and K. Van Laerhoven, "A scoping review of gaze and eye tracking-based control methods for assistive robotic arms," *Frontiers in Robotics and AI*, vol. 11, no. 2, Feb. 2024, doi: 10.3389/frobt.2024.1326670.

[30] D. Kang and J. Heo, "Content-Aware Eye Tracking for Autostereoscopic 3D Display," *Sensors*, vol. 20, no. 17, p. 4787, Aug. 2020, doi: 10.3390/s20174787.

[31] Y. Lei, S. He, M. Khamis, and J. Ye, "An End-to-End Review of Gaze Estimation and its Interactive Applications on Handheld Mobile Devices," *ACM Computing Surveys*, vol. 56, no. 2, pp. 1–38, Feb. 2024, doi: 10.1145/3606947.

[32] M. S. A. bin Suhaimi, K. Matsushita, T. Kitamura, P. W. Laksono, and M. Sasaki, "Object Grasp Control of a 3D Robot Arm by Combining EOG Gaze Estimation and Camera-Based Object Recognition," *Biomimetics*, vol. 8, no. 2, p. 208, May 2023, doi: 10.3390/biomimetics8020208.

[33] E. H. E. Suryadarma, P. W. Laksono, I. Priadythama, and L. Herdiman, "Controlling Robots Using Gaze Estimation: A Systematic Bibliometric and Research Trend Analysis," *Journal of Robotics and Control (JRC)*, vol. 5, no. 3, pp. 786–803, 2024, doi: 10.18196/jrc.v5i3.21686.

[34] R. Hunt, T. Blackmore, C. Mills, and M. Dicks, "Evaluating the integration of eye-tracking and motion capture technologies: Quantifying the accuracy and precision of gaze measures," *i-Perception*, vol. 13, no. 5, 2022, doi: 10.1177/20416695221116652.

[35] J. M. Araujo, G. Zhang, J. P. P. Hansen, and S. Puthusserypady, "Exploring Eye-Gaze Wheelchair Control," 2020, doi: 10.1145/3379157.3388933.

[36] P. Pathirana, S. Senarath, D. Meedeniya, and S. Jayarathna, "Eye gaze estimation: A survey on deep learning-based approaches," *Expert Systems with Applications*, vol. 199, p. 116894, Aug. 2022, doi: 10.1016/j.eswa.2022.116894.

[37] A. A. Akinyelu and P. Blignaut, "Convolutional Neural Network-Based Methods for Eye Gaze Estimation: A Survey," *IEEE Access*, vol. 8, pp. 142581–142605, 2020, doi: 10.1109/ACCESS.2020.3013540.

[38] Á. Miklósi and M. Gácsi, "On the Utilization of Social Animals as a Model for Social Robotics," *Frontiers in Psychology*, vol. 3, no. 3, 2012, doi: 10.3389/fpsyg.2012.00075.

[39] L. Almeida, P. Menezes, and J. Dias, "Telepresence Social Robotics towards Co-Presence: A Review," *Applied Sciences*, vol. 12, no. 11, p. 5557, May 2022, doi: 10.3390/app12115557.

[40] A. Sharkey and N. Sharkey, "We need to talk about deception in social robotics," *Ethics and Information Technology*, vol. 23, no. 3, pp. 309–316, Sep. 2021, doi: 10.1007/s10676-020-09573-9.

[41] M. Capasso, "Responsible Social Robotics and the Dilemma of Control," *International Journal of Social Robotics*, vol. 15, no. 12, pp. 1981–1991, Dec. 2023, doi: 10.1007/s12369-023-01049-2.

[42] R. Martinez-Roig, M. Cazorla, and J. M. Esteve Faubel, "Social robotics in music education: A systematic review," *Frontiers in Education*, vol. 8, no. 3, Mar. 2023, doi: 10.3389/feduc.2023.1164506.

[43] K. Youssef, S. Said, S. Alkork, and T. Beyrouthy, "A Survey on Recent Advances in Social Robotics," *Robotics*, vol. 11, no. 4, p. 75, Jul. 2022, doi: 10.3390/robotics11040075.

[44] N. Akalin and A. Loutfi, "Reinforcement Learning Approaches in Social Robotics," *Sensors*, vol. 21, no. 4, p. 1292, Feb. 2021, doi: 10.3390/s21041292.

[45] G. Zhang, J. P. Hansen, and K. Minakata, "Hand- and gaze-control of telepresence robots," in *Proceedings of the 11th ACM Symposium on Eye Tracking Research & Applications*, pp. 1–8, Jun. 2019, doi: 10.1145/3317956.3318149.

[46] I. T. C. Hooge, G. A. Holleman, N. C. Haukes, and R. S. Hessels, "Gaze tracking accuracy in humans: One eye is sometimes better than two," *Behavior Research Methods*, vol. 51, no. 6, pp. 2712–2721, Dec. 2019, doi: 10.3758/s13428-018-1135-3.

[47] E. Lambe and P. Cuffe, "Design and Test of a Headset Activation Platform Controlled by Eye Gaze Tracking," in *IECON 2019 - 45th Annual Conference of the IEEE Industrial Electronics Society*, pp. 5364–5369, Oct. 2019, doi: 10.1109/IECON.2019.8927716.

[48] V. V and S. R. Gopal, "Applications of Robotics in Healthcare," *International Journal of Scientific Research in Engineering and Management (IJSREM)*, vol. 06, no. 06, Jun. 2022, doi: 10.55041/IJSREM14231.

[49] C. Elendu *et al.*, "Ethical implications of AI and robotics in healthcare: A review," *Medicine*, vol. 102, no. 50, p. e36671, Dec. 2023, doi: 10.1097/MD.0000000000036671.

[50] E. Kamani, D. E. Kalisz, and A. Szyran-Resiak, "Patients' behavioral intentions toward robotic adoption in healthcare: An approach on apprehension of embedding robotics," *Journal of General Management*, vol. 48, no. 4, pp. 370–385, Jul. 2023, doi: 10.1177/03063070221080008.

[51] D. Silvera-Tawil, "Robotics in Healthcare: A Survey," *SN Computer Science*, vol. 5, no. 1, p. 189, 2024, doi: 10.1007/s42979-023-02551-0.

[52] M. Solberg and R. Kirchhoff, "Media Representations of Healthcare Robotics in Norway 2000-2020: A Topic Modeling Approach," *Social*

Science Computer Review, vol. 42, no. 3, pp. 636–660, Jun. 2024, doi: 10.1177/08944393231212251.

[53] G. Mois and J. M. Beer, "The Role of Healthcare Robotics in Providing Support to Older Adults: a Socio-ecological Perspective," *Current Geriatrics Reports*, vol. 9, no. 2, pp. 82–89, Mar. 2020, doi: 10.1007/s13670-020-00314-w.

[54] S. Breuer, M. Braun, D. Tigard, A. Buyx, and R. Müller, "How Engineers' Imaginaries of Healthcare Shape Design and User Engagement: A Case Study of a Robotics Initiative for Geriatric Healthcare AI Applications," *ACM Transactions on Computer-Human Interaction*, vol. 30, no. 2, pp. 1–33, Apr. 2023, doi: 10.1145/3577010.

[55] C. Anthes, R. J. Garcia-Hernandez, M. Wiedemann, and D. Kranzlmuller, "State of the art of virtual reality technology," in *2016 IEEE Aerospace Conference*, pp. 1–19, Mar. 2016, doi: 10.1109/AERO.2016.7500674.

[56] S. Pastel, C.-H. Chen, L. Martin, M. Naujoks, K. Petri, and K. Witte, "Comparison of gaze accuracy and precision in real-world and virtual reality," *Virtual Reality*, vol. 25, no. 1, pp. 175–189, Mar. 2021, doi: 10.1007/s10055-020-00449-3.

[57] G. Zhang and J. P. Hansen, "A Virtual Reality Simulator for Training Gaze Control of Wheeled Tele-Robots," in *25th ACM Symposium on Virtual Reality Software and Technology*, pp. 1–2, Nov. 2019, doi: 10.1145/3359996.3364707.

[58] R. Guo, Y. Lin, X. Luo, X. Gao, and S. Zhang, "A robotic arm control system with simultaneous and sequential modes combining eye-tracking with steady-state visual evoked potential in virtual reality environment," *Frontiers in Neurorobotics*, vol. 17, Mar. 2023, doi: 10.3389/fnbot.2023.1146415.

[59] A. Matsuzaka, L. Yang, C. Guo, T. Shirato, and A. Namiki, "Assistance for Master-Slave System for Objects of Various Shapes by Eye Gaze Tracking and Motion Prediction," in *2018 IEEE International Conference on Robotics and Biomimetics (ROBIO)*, pp. 1953–1958, Dec. 2018, doi: 10.1109/ROBIO.2018.8664898.

[60] Y. F. Wu and E. Y. Kim, "Users' Perceptions of Technological Features in Augmented Reality (AR) and Virtual Reality (VR) in Fashion Retailing: A Qualitative Content Analysis," *Mobile Information Systems*, vol. 2022, pp. 1–13, Aug. 2022, doi: 10.1155/2022/3080280.

[61] D. Kanschik, R. R. Bruno, G. Wolff, M. Kelm, and C. Jung, "Virtual and augmented reality in intensive care medicine: a systematic review," *Annals of Intensive Care*, vol. 13, no. 1, p. 81, Sep. 2023, doi: 10.1186/s13613-023-01176-z.

[62] S. Kim, S. Lee, H. Kang, S. Kim, and M. Ahn, "P300 Brain–Computer Interface-Based Drone Control in Virtual and Augmented Reality," *Sensors*, vol. 21, no. 17, p. 5765, Aug. 2021, doi: 10.3390/s21175765.

[63] N. Dzyuba, J. Jandu, J. Yates, and E. Kushnerev, "Virtual and augmented reality in dental education: The good, the bad and the better," *European Journal of Dental Education*, Nov. 2022, doi: 10.1111/eje.12871.

[64] Y.-C. Lin *et al.*, "Combining augmented and virtual reality simulation training to improve geriatric oral care performance in healthcare assistants: A randomized controlled trial," *DIGITAL HEALTH*, vol. 9, Jan. 2023, doi: 10.1177/20552076231203891.

[65] P. Bhattacharya *et al.*, "Coalition of 6G and Blockchain in AR/VR Space: Challenges and Future Directions," *IEEE Access*, vol. 9, pp. 168455–168484, 2021, doi: 10.1109/ACCESS.2021.3136860.

[66] F. Ke, R. Liu, Z. Sokolikj, I. Dahlstrom-Hakki, and M. Israel, "Using eye-tracking in education: review of empirical research and technology," *Educational technology research and development*, vol. 72, no. 3, pp. 1383–1418, Jun. 2024, doi: 10.1007/s11423-024-10342-4.

[67] J. Y. Kim and M. J. Kim, "Identifying customer preferences through the eye-tracking in travel websites focusing on neuromarketing," *Journal of Asian Architecture and Building Engineering*, vol. 23, no. 2, pp. 515–527, Mar. 2024, doi: 10.1080/13467581.2023.2244566.

[68] J. Linde-Domingo and B. Spitzer, "Geometry of visuospatial working memory information in miniature gaze patterns," *Nature Human Behaviour*, vol. 8, no. 2, pp. 336–348, Dec. 2023, doi: 10.1038/s41562-023-01737-z.

[69] L. R. Lidle and J. Schmitz, "Assessing Visual Avoidance of Faces During Real-Life Social Stress in Children with Social Anxiety Disorder: A Mobile Eye-Tracking Study," *Child Psychiatry & Human Development*, vol. 55, no. 1, pp. 24–35, Feb. 2024, doi: 10.1007/s10578-022-01383-y.

[70] T. Suslow, D. Hoepfel, A. Kersting, and C. M. Bodenschatz, "Depressive symptoms and visual attention to others' eyes in healthy individuals," *BMC Psychiatry*, vol. 24, no. 1, p. 184, Mar. 2024, doi: 10.1186/s12888-024-05633-2.

[71] M. S. H. Sunny *et al.*, "Eye-gaze control of a wheelchair mounted 6DOF assistive robot for activities of daily living," *Journal of NeuroEngineering and Rehabilitation*, vol. 18, no. 1, p. 173, Dec. 2021, doi: 10.1186/s12984-021-00969-2.

[72] A. McCurley and D. Nathan-Roberts, "Eye-Tracking Assistive Technology for Hands-Free Computer Navigation," *Proceedings of the Human Factors and Ergonomics Society Annual Meeting*, vol. 65, no. 1, pp. 1275–1279, Sep. 2021, doi: 10.1177/1071181321651313.

[73] M. Donmez, "A systematic literature review for the use of eye-tracking in special education," *Education and Information Technologies*, vol. 28, no. 6, pp. 6515–6540, Jun. 2023, doi: 10.1007/s10639-022-11456-z.

[74] C. Leblond-Menard and S. Achiche, "Non-Intrusive Real Time Eye Tracking Using Facial Alignment for Assistive Technologies," *IEEE Transactions on Neural Systems and Rehabilitation Engineering*, vol. 31, pp. 954–961, 2023, doi: 10.1109/TNSRE.2023.3236886.

[75] H. O. Edughele, Y. Zhang, F. Muhammad-Sukki, Q.-T. Vien, H. Morris-Cafiero, and M. Opoku Agyeman, "Eye-Tracking Assistive Technologies for Individuals With Amyotrophic Lateral Sclerosis," *IEEE Access*, vol. 10, pp. 41952–41972, 2022, doi: 10.1109/ACCESS.2022.3164075.

[76] W. Rahmaniar, A. Ma'Arif, and T.-L. Lin, "Touchless Head-Control (THC): Head Gesture Recognition for Cursor and Orientation Control," *IEEE Transactions on Neural Systems and Rehabilitation Engineering*, vol. 30, pp. 1817–1828, 2022, doi: 10.1109/TNSRE.2022.3187472.

[77] J. K. Muguro *et al.*, "Development of Surface EMG Game Control Interface for Persons with Upper Limb Functional Impairments," *Signals*, vol. 2, no. 4, pp. 834–851, Nov. 2021, doi: 10.3390/signals2040048.

[78] T. Faibish, A. Kshirsagar, G. Hoffman, and Y. Edan, "Human Preferences for Robot Eye Gaze in Human-to-Robot Handovers," *International Journal of Social Robotics*, vol. 14, no. 4, pp. 995–1012, 2022, doi: 10.1007/s12369-021-00836-z.

[79] S. K. Paul, M. Nicolescu, and M. Nicolescu, "Enhancing Human–Robot Collaboration through a Multi-Module Interaction Framework with Sensor Fusion: Object Recognition, Verbal Communication, User of Interest Detection, Gesture and Gaze Recognition," *Sensors*, vol. 23, no. 13, p. 5798, Jun. 2023, doi: 10.3390/s23135798.

[80] R. T. Chadalavada, H. Andreasson, M. Schindler, R. Palm, and A. J. Lilienthal, "Bi-directional navigation intent communication using spatial augmented reality and eye-tracking glasses for improved safety in human–robot interaction," *Robotics and Computer-Integrated Manufacturing*, vol. 61, p. 101830, Feb. 2020, doi: 10.1016/j.rcim.2019.101830.

[81] F. Babel *et al.*, "Small Talk with a Robot? The Impact of Dialog Content, Talk Initiative, and Gaze Behavior of a Social Robot on Trust, Acceptance, and Proximity," *International Journal of Social Robotics*, vol. 13, no. 6, pp. 1485–1498, Sep. 2021, doi: 10.1007/s12369-020-00730-0.

[82] J. Muguro, P. W. Laksono, Y. Sasatake, M. I. Rusydi, K. Matsushita, and M. Sasaki, "Feasibility of AR-VR use in autonomous cars for user engagements and its effects on posture and vigilance during transit," *Transactions on Transport Sciences*, vol. 14, no. 1, pp. 4–13, Apr. 2023, doi: 10.5507/tots.2022.019.

[83] J. K. Muguro, P. W. Laksono, Y. Sasatake, K. Matsushita, and M. Sasaki, "User Monitoring in Autonomous Driving System Using Gamified Task: A Case for VR/AR In-Car Gaming," *Multimodal Technologies and Interaction*, vol. 5, no. 8, p. 40, Jul. 2021, doi: 10.3390/mti5080040.

[84] Z. Zhan, J. Wu, H. Mei, Q. Wu, and P. S. W. Fong, "Individual difference on reading ability tested by eye-tracking: from perspective of gender," *Interactive Technology and Smart Education*, vol. 17, no. 3, pp. 267–283, Mar. 2020, doi: 10.1108/ITSE-12-2019-0082.

[85] J. Chen, P. Yu, C. Yao, L. Zhao, and Y. Qiao, "Eye detection and coarse localization of pupil for video-based eye tracking systems," *Expert*

Systems with Applications, vol. 236, p. 121316, Feb. 2024, doi: 10.1016/j.eswa.2023.121316.

[86] W. Liu, Y. Cao, and R. W. Proctor, "How do app icon color and border shape influence visual search efficiency and user experience? Evidence from an eye-tracking study," *International Journal of Industrial Ergonomics*, vol. 84, p. 103160, Jul. 2021, doi: 10.1016/j.ergon.2021.103160.

[87] Z. Xun *et al*., "Eye behavior recognition of eye–computer interaction," *Multimedia Tools and Applications*, vol. 83, no. 11, pp. 32655–32671, Sep. 2023, doi: 10.1007/s11042-023-16763-2.

[88] A. Zafar, C. M. Calderon, A. M. Yeboah, K. Dalton, E. Irving, and E. Niechwiej-Szwedo, "Investigation of Camera-Free Eye-Tracking Glasses Compared to a Video-Based System," *Sensors*, vol. 23, no. 18, p. 7753, Sep. 2023, doi: 10.3390/s23187753.

[89] J. Lyu and F. Xu, "Towards Eyeglasses Refraction in Appearance-based Gaze Estimation," in *2023 IEEE International Symposium on Mixed and Augmented Reality (ISMAR)*, pp. 693–702, Oct. 2023, doi: 10.1109/ISMAR59233.2023.00084.

[90] J. W. Lee, C. W. Cho, K. Y. Shin, E. C. Lee, and K. R. Park, "3D gaze tracking method using Purkinje images on eye optical model and pupil," *Optics and Lasers in Engineering*, vol. 50, no. 5, pp. 736–751, May 2012, doi: 10.1016/j.optlaseng.2011.12.001.

[91] X. Xu, L. Yang, Y. Yan, and C. Li, "CMFS-Net: Common Mode Features Suppression Network for Gaze Estimation," in *Proceedings of the 2023 Workshop on Advanced Multimedia Computing for Smart Manufacturing and Engineering*, pp. 25–29, Oct. 2023, doi: 10.1145/3606042.3616449.

[92] M. Othman, T. Amaral, R. McNaney, J. D. Smeddinck, J. Vines, and P. Olivier, "CrowdEyes," in *Proceedings of the 19th International Conference on Human-Computer Interaction with Mobile Devices and Services*, pp. 1–13, Sep. 2017, doi: 10.1145/3098279.3098559.